JPNT 4(3), 97-105 (2015)
http://dx.doi.org/10.11003/JPNT.2015.4.3.097

JPNT Journal of Positioning, Navigation, and Timing

Navigation Signals Based on Orthogonal Tiered Polyphase Code

Jewon Lee[1], Jeong-been Kim[2], Kap-jin Kim[3], Ki-won Song[3], Jae Min Ahn[1†]

[1]Department of Information and communication, Chungnam National University, Daejeon 305-764, Korea
[2]Korea Institute of Patent Information Patent Information Promotion Center, Daejeon 302-859, Korea
[3]Agency for Defense Development, Daejeon 305-764, Korea

ABSTRACT

A navigation signal based on orthogonal tiered polyphase code was proposed. For the proposed signal, tiered polyphase code was used as the code of a pilot channel. Tiered polyphase code is a complex number type code, and thus the pilot channel and data channel were separated using the Walsh code which makes the correlation between different codes become 0. The results of the simulation indicated that the correlation characteristics and signal acquisition performance of the proposed signal were identical to those of tiered polyphase code, and that the disadvantage of tiered polyphase code could be supplemented through a data channel in terms of signal tracking.

Keywords: tiered polyphase code, walsh code, signal acquisition, frequency offset estimation

1. INTRODUCTION

For the Global Navigation Satellite System (GNSS), one of the major issues is the design of ranging code. Global Positioning System (GPS) (Dunn 2013), GALILEO (European Union 2010), and BeiDou (China Satellite Navigation Office 2013) have a tiered code structure that consists of a primary code and a secondary code. A tiered code structure is used in GNSS because it has advantages compared to an existing code structure in terms of signal acquisition/tracking and data demodulation.

A GPS L5 signal consists of a data channel and a pilot channel. For the secondary code, the data channel uses Neuman Hoffman (NH) with a length of 10 (NH_{10}=0000110101), and the pilot channel uses NH with a length of 20 (NH_{20}=00000100110101001110). The secondary code of BeiDou also uses NH code with a length of 20, which is identical to that of GPS L5. When NH code is used, the signal becomes robust to narrowband interference. This is because the power of narrowband interference can be decreased by 10 or 13 dB through the despreading of NH code. Also, when the correlation of primary code length is performed with and without NH code, the auto- and cross-correlation side peak protection margins can be additionally obtained by 0.4 and 1.7 dB, respectively, when NH code is used. Lastly, the data bit synchronization performance can be improved. However, NH20 code is vulnerable to frequency offset as the difference between the maximum value and the second maximum value is 2.59 dB in an environment with a frequency offset of 30 Hz. To overcome this problem, various studies have been performed (Yang et al. 2004, Zou et al. 2009).

Kim et al. (2014) suggested Tiered Polyphase Code (TPC) by replacing a secondary code with the Zadoff-Chu sequence in the signal structure of GALILEO E5a-I. The Zadoff-Chu sequence has Constant Amplitude Zero Auto Correlation and robust to frequency error. It was demonstrated that when the same Zadoff-Chu sequence was used as a secondary code for all satellites, there was no cross-correlation interference when the transmitted signals between the satellites were apart by more than the length of the primary code. In addition, Kim & Ahn (2013) showed that when the primary code epoch rate was 1 kHz,

Received July 28, 2015 **Revised** Aug 19, 2015 **Accepted** Aug 25, 2015
†**Corresponding Author**
E-mail: jmahn@cnu.ac.kr
Tel: +82-42-821-7796 Fax: +82-42-823-5586

http://www.gnss.or.kr Print ISSN: 2288-8187 Online ISSN: 2289-0866

signal acquisition was possible without frequency offset compensation in an environment with a frequency offset of 700 Hz. However, the Zadoff-Chu sequence is a complex number type code, and thus the index of the maximum correlation value is affected by time delay and frequency offset. In other words, the starting position of a primary code can be found from the obtained signal, but the starting position of a secondary code can be accurately known only when the frequency offset is precisely estimated.

In the case of TPC, the starting position of a secondary code cannot be known after signal acquisition, and thus there is difficulty in the frequency estimation method using a primary code. To estimate frequency using a secondary code, a method in which all the 20 secondary code values are substituted needs to be used. Thus, the complexity increases, and the range in which frequency offset estimation is possible is also limited. To overcome this limitation, a new signal structure is needed.

In this study, the experiment results for the navigation signal based on orthogonal Tiered Polyphase Code (OTPC) and the signal acquisition and frequency estimation methods suggested by Kim (2014) were theoretically analyzed. Also, an additional experiment was performed for the frequency estimation method, and the results were presented. TPC is a complex number type code. Thus, to use TPC as the code of a pilot channel, a method that is different from the method in which a data channel and a pilot channel are sent by dividing them into in-phase and quadrature in an existing navigation system is required. For the suggested navigation signal, a data channel and a pilot channel were separated using an orthogonal code (e.g., Walsh code) which makes the correlation between different codes become 0. The results of the simulation indicated that the advantage of existing TPC was maintained during signal acquisition, and signal tracking was possible as precise frequency offset estimation was enabled using a data channel.

In Chapter 2, the frequency estimation method using TPC and the limitations were presented; and in Chapter 3, a navigation signal structure where TPC is used as the code of a pilot channel was proposed. In Chapter 4, the correlation characteristics and signal acquisition performance of the proposed signal and the frequency estimation method and performance using a data channel were examined; and conclusions were included in Chapter 5.

2. FREQUENCY OFFSET ESTIMATION LIMITS OF TIERED POLYPHASE CODE

In the tiered code (TC) used for GALILEO E5a-I, the chip rates of the primary code and secondary code are 10.23 MHz and 1 kHz, respectively, and the code lengths are 10230 and 20, respectively. TPC where the secondary code was replaced with the Zadoff-Chu sequence in the TC of GALILEO E5a-I is appropriate for a satellite navigation signal system because it has no interference effect between satellite signals constituting the same system and is robust to frequency offset. However, the starting position of a primary code that is received at 1 ms intervals through signal acquisition can be accurately known; but to figure out the starting position of a secondary code that is repeated at 20 ms intervals, frequency offset needs to be accurately estimated. However, in the case of polyphase code, the code is a complex number and has a phase component. Thus, if the starting position is not known, there is a limit in estimating the phase component added to the continuous primary code. Eq. (1) expresses a received signal that has been received with a frequency offset defined for frequency offset estimation.

$$\begin{aligned} S(n) &= \exp\left(j\frac{\pi n^2}{20}\right)\cdot\exp\left(j2\pi\Delta f t\right),\ t=\frac{n}{1000},\ n=0,\ 1,\ \ldots,\ 19 \\ &= \exp\left(j\frac{\pi n^2}{20}\right)\cdot\exp\left(\frac{j2\pi\Delta f n}{1000}\right) \end{aligned} \tag{1}$$

where the first exponential term is the Zadoff-Chu sequence, and it changes depending on the order of the primary code constituting the received TPC. The second exponential term is the frequency offset. The term for the despreading process using the Zadoff-Chu sequence for the received signal is expressed in Eq. (2), and the despreading process is expressed in Eq. (3).

$$\exp\left(-j\frac{\pi(n-k)^2}{20}\right) \tag{2}$$

$$\begin{aligned} R_k(n) &= S(n)\times\exp\left(-j\frac{\pi(n-k)^2}{20}\right) \\ &= \exp\left(j\frac{\pi n^2+2\pi\cdot\frac{\Delta f}{50}n}{20}\right)\times\exp\left(-j\frac{\pi(n-k)^2}{20}\right) \\ &= \exp\left[j\left(\frac{\pi n^2+2\pi\cdot\frac{\Delta f}{50}n}{20}\right)-j\left(\frac{\pi n^2-2\pi nk+\pi k^2}{20}\right)\right] \\ &= \exp\left[j\frac{2\pi nk+2\pi\frac{\Delta f}{50}n-\pi k^2}{20}\right]=\exp\left[j\frac{2\pi n\left(k+\frac{\Delta f}{50}\right)}{20}\right]\cdot\exp\left[-j\frac{\pi k^2}{20}\right] \end{aligned} \tag{3}$$

where n is the code index, and k represents the polyphase code set shown in Fig. 1 which is the set of secondary codes that can be applied to the corresponding time. For example, in the case of $k=0$, despreading for the received signal is performed using secondary codes whose secondary code

http://dx.doi.org/10.11003/JPNT.2015.4.3.097

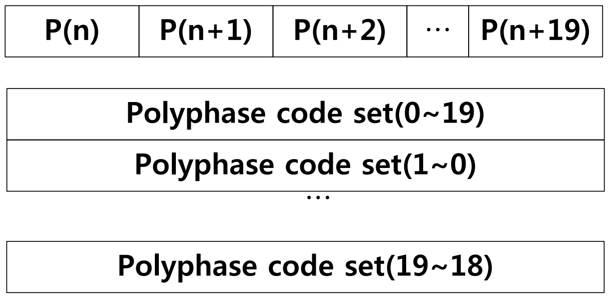

Fig. 1. Frequency offset estimation method of TPC.

indices are 0, 1,...,18,19; and in the case of $k=1$, despreading for the received signal is performed using secondary codes whose secondary code indices are 1,2,...,19,0. When the despread received signal goes through the delay and multiply process for obtaining frequency offset, it can be expressed as Eq. (4).

$$R_k^*(n-1)R_k(n) = \exp\left[-j\frac{2\pi(n-1)\left(k+\frac{\Delta f}{50}\right)}{20}\right]\cdot\left[j\frac{2\pi n\left(k+\frac{\Delta f}{50}\right)}{20}\right] = \exp\left[j\frac{2\pi\left(k+\frac{\Delta f}{50}\right)}{20}\right] \quad (4)$$

However, among the 20 primary codes constituting TPC, the position at which the received signal is located cannot be known, and thus a method in which all the 20 secondary code values are substituted needs to be used as shown in Fig. 1.

The process for obtaining the frequency offset component, Δf, based on the result of Eq. (4) as shown in Fig. 1 can be expressed as Eq. (5).

$$\begin{aligned}\prod_{k=0}^{19} R_k^*(n-1)R_k(n) &= \prod_{k=0}^{19}\exp\left[j\frac{2\pi\left(k+\frac{\Delta f}{50}\right)}{20}\right]\\ &= \exp\left[j\sum_{k=0}^{19}\left(\frac{2\pi}{20}k+\frac{2\pi}{20}\cdot\frac{\Delta f}{50}\right)\right] = \exp\left[j\sum_{k=0}^{19}\left(\frac{2\pi}{20}k\right)+j2\pi\cdot\frac{\Delta f}{50}\right]\\ &= \exp\left[j2\pi\cdot\frac{\Delta f}{50}\right]\cdot\exp\left[j\frac{\pi}{10}\cdot 190\right],\ \exp[j19\pi]=-1\\ &= -\exp\left[j2\pi\cdot\frac{\Delta f}{50}\right] = C_i + jC_q \end{aligned} \quad (5)$$

For a complex number which is the result of Eq. (5), the phase can be obtained using an arctangent function, etc.; and based on this, frequency offset can be accurately estimated. However, if a wide integration interval of 20 ms is used for this method, estimation is impossible because the phase rotates more than 180 degrees when there is a frequency offset of more than ±25 Hz as shown in the frequency offset term of the result of Eq. (5).

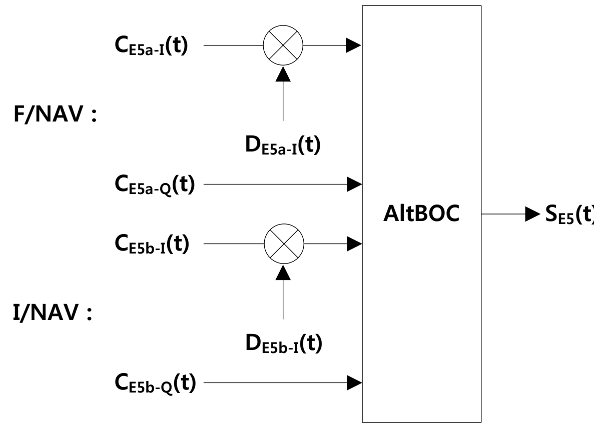

Fig. 2. Signal structure of GALILEO E5.

3. NAVIGATION SIGNAL BASED ON TIERED POLYPHASE CODE

Most currently developed satellite navigation signal systems including GALILEO from the European Union consist of a pilot channel that can bring accurate correlation values at regular intervals and a data channel that is transmitted at the same intervals or at a period of integer multiple and sends information such as navigation message. In the case of the GALILEO E5 service shown in Fig. 2, E5a transmits an F/NAV message that supports the GALILEO Open service, and E5b transmits an I/NAV message that supports the Safety of Life service, GALILEO system integrity, and Open service. Each message, D, is multiplied by the ranging code of the in-phase axis of the complex plane, forming a data channel; and is multiplied by the ranging code of the quadrature axis, forming a pilot channel. They are then transmitted at the same time using the AltBOC modulation technique.

As mentioned above, the pilot/data channels of a general satellite navigation system transmits data generated through the in-phase/quadrature channels, respectively. However, in the case of TPC, channels cannot be divided based on this method since the polyphase code consists of a complex number. Therefore, for the navigation signal based on TPC proposed in this study, a data channel is generated and transmitted using an orthogonal code which makes the cross-correlation between different codes become 0, such as the Walsh code which is used in the code division multiple access technique. Fig. 3 shows the navigation signal generation method using TPC.

As shown in Fig. 3, existing TPC is used for a pilot channel, and the primary code repeated by the N_p unit is multiplied by the orthogonal code with the same length and by the data repeated at N_pN_s intervals. Then, a data channel

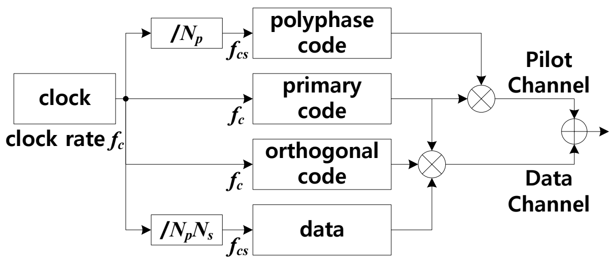

Fig. 3. Signal structure based on TPC.

is added, and they are transmitted through the pilot/data channels. Another advantage of using a signal system where pilot and data channels are divided is that frequency offset can be estimated in a synchronization process through the data channel. When a signal is first acquired through the pilot channel and accurate period of the primary code is obtained, frequency offset can be estimated using the data channel with the use of the delay and multiply process which is a general frequency offset estimation algorithm. Additionally, a technique that can precisely estimate the frequency offset component within a ±25 Hz range explained in Chapter 2 can also be used.

4. SIMULATION

Table 1 summarizes the parameters of the OTPC for the simulation.

4.1 Signal Acquisition

For the TPC of the proposed navigation signal, pilot and data channels are separated through an orthogonal code. Thus, in the presence of this orthogonality, it needs to be examined if the received signal of the pilot channel shows characteristics that are the same as when only TPC exists.

$$\begin{aligned} &\frac{1}{N}\sum_{i=0}^{N-1}\left|C_p(i)\right|^2 \times C_o(i) = 0, \text{ Pilot channel} \\ &\frac{1}{N}\sum_{i=0}^{N-1}\left|C_p(i)\right|^2 \times \left|C_o(i)\right|^2 = 1, \text{ Data channel} \end{aligned} \tag{6}$$

where C_p is the primary code, C_0 is the orthogonal code, and N is the length of the primary and orthogonal code. As the relationship shown in Eq. (6) is valid, when a despreading process is performed for the code generated in Fig. 3 using the primary code, the TPC component of the pilot channel can be obtained. Also, when this is multiplied by an orthogonal code, the component of the data channel can be obtained.

When a number of satellite signals constituting the same system are received with a time delay, the primary code of the k-th satellite, $C_{p,k}$, can be expressed as Eq. (7), the secondary code that is commonly applied to all the satellites, C_S, can be expressed as Eq. (8), and the data of the k-th satellite, D_k, can be expressed as Eq. (9).

Table 1. Simulation parameters.

Component	Code	Rate (MHz)	Length (chips)	Period (ms)
Primary code	Gold likely code	10.23	10230	1
Secondary code	Zadoff-Chu sequnece	0.001	20	20
Orthogonal code	Walsh code	10.23	10230	1

$$C_{p,k}(n) = 0, \text{ for } n < 0 \text{ or } n \geq N_p \tag{7}$$

$$C_s(n) = \sum_{v=0}^{N_s-1} m(v)\delta(n - vN_p) \tag{8}$$

$$D_k(n) = \sum_{\ell=0}^{\infty} d_k(\ell)\delta(n - \ell N_p N_s) \tag{9}$$

where N_p is the length of the primary code, N_s is the length of the secondary code, $m(v)$ is the value of the secondary code, and $d_k(l)$ is the data of the k-th satellite. Eq. (10) expresses the transmitted signal of the k-th satellite, S_k.

$$\begin{aligned} S_k(n) &= C_{p,k}(n) * C_s(n) + C_{p,k}(n)C_o(n) * D_k(n) \\ &= C_{p,k}(n) * \sum_{v=0}^{N_s-1} m(v)\delta(n - vN_p) + C_{p,k}(n)C_o(n) * \sum_{\ell=0}^{\infty} d_k(\ell)\delta(n - \ell N_p N_s) \\ &= \sum_{v=0}^{N_s-1} m(v)C_{p,k}(n - vN_p) + \sum_{\ell=0}^{\infty} d_k(\ell)C_{p,k}C_o(n - \ell N_p N_s) \end{aligned} \tag{10}$$

where C_0 is the orthogonal code that is commonly applied to all the satellites. The receiver input signal can be expressed as Eq. (11).

$$r(n) = \sum_{k=1}^{K} S_k(n - \lambda_k) \tag{11}$$

where k is the number of satellites, and λ_k is the simplex time delay of the received satellite signal. When a correlation for Eq. (11) and the primary code of satellite 1 is performed, it can be expressed as Eq. (12).

$$\begin{aligned} V_1(\tau) &= \sum_{n=0}^{N_p-1} r(n+\tau) \cdot C_{p,1}^*(n) \\ &= \sum_{n=0}^{N_p-1}\left[\sum_{k=1}^{K} S_k(n + \tau - \lambda_k)\right] \cdot C_{p,1}^*(n) \\ &= \sum_{k=1}^{K}\sum_{v=0}^{N_s-1} m(v) \underline{\sum_{n=0}^{N_p-1} C_{p,k}(n + \tau - \lambda_k - vN_p) \cdot C_{p,1}^*(n)} \\ &+ \sum_{k=1}^{K}\sum_{\ell=0}^{\infty} d_k(\ell) \sum_{n=0}^{N_p-1} C_o C_{p,k}(n + \tau - \lambda_k - \ell N_p N_s) \cdot C_{p,1}^*(n) \end{aligned} \tag{12}$$

According to the definition of Eq. (7), there are only two consecutive v values where the term underlined in Eq. (12) is not 0, as shown in Fig. 4 ($v_{k,\tau}$ and $v_{k,\tau}+1$).

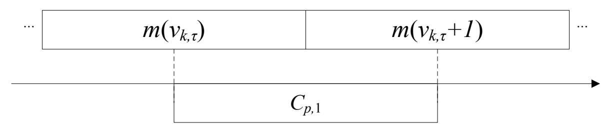

Fig. 4. Correlation process using primary code.

Thus, Eq. (12) can be arranged as shown in Eq. (13).

$$V_1(\tau)=\sum_{k=1}^{K}\left[\begin{array}{l} m\left(v_{k,\tau}\right)\sum_{n=0}^{N_p-1}C_{p,k}\left(n+\tau-\lambda_k-v_{k,\tau}N_p\right)\cdot C_{p,1}^{*}(n) \\ +m\left(v_{k,\tau}+1\right)\sum_{n=0}^{N_p-1}C_{p,k}\left(n+\tau-\lambda_k-\left(v_{k,\tau}+1\right)N_p\right)\cdot C_{p,1}^{*}(n) \\ +\sum_{\ell=0}^{\infty}d_k(\ell)\sum_{n=0}^{N_p-1}C_oC_{p,k}\left(n+\tau-\lambda_k-\ell N_pN_s\right)\cdot C_{p,1}^{*}(n) \end{array}\right] \quad (13)$$

In this regard, $0\leq n+\tau-\lambda_k-v_{k,\tau}N_p<N_p$ needs to be satisfied, and thus it is as follows.

$$\begin{aligned} & n+\tau-\lambda_k-v_{k,\tau}N_p \\ & =n+\left(\tau-\lambda_k-v_{k,\tau}N_p\right)\bmod N_p \\ & =n+\left(\tau-\lambda_k\right)\bmod N_p \end{aligned} \quad (14)$$

Based on Eq. (14), Eq. (13) can be arranged as follows.

$$\begin{aligned} & \sum_{n=0}^{N_p-1}C_{p,k}\left(n+\tau-\lambda_k-v_{k,\tau}N_p\right)\cdot C_{p,1}^{*}(n) \\ & =\sum_{n=0}^{N_p-1}C_{p,k}\left(n+(\tau-\lambda_k)\bmod N_p\right)\cdot C_{p,1}^{*}(n) \\ & \triangleq R_{p,k1}^{l}\left((\tau-\lambda_k)\bmod N_p\right) \end{aligned} \quad (15)$$

$$\begin{aligned} & \sum_{n=0}^{N_p-1}C_{p,k}\left(n+\tau-\lambda_k-\left(v_{k,\tau}+1\right)N_p\right)\cdot C_{p,1}^{*}(n) \\ & =\sum_{n=0}^{N_p-1}C_{p,k}\left(n+(\tau-\lambda_k)\bmod N_p-N_p\right)\cdot C_{p,1}^{*}(n) \\ & \triangleq R_{p,k1}^{r}\left((\tau-\lambda_k)\bmod N_p-N_p\right) \end{aligned} \quad (16)$$

$$\begin{aligned} & \sum_{n=0}^{N_p-1}C_oC_{p,k}\left(n+\tau-\lambda_k-\ell N_pN_s\right)\cdot C_{p,1}^{*}(n) \\ & =\sum_{n=0}^{N_p-1}C_oC_{p,k}\left(n+\tau-\lambda_k-\ell N_pN_s\right)\cdot C_{p,1}^{*}(n) \\ & \triangleq P_{d,k1}\left(\left(\tau-\lambda_k\right)\bmod N_p\right) \end{aligned} \quad (17)$$

$$V_1(\tau)=\sum_{k=1}^{K}\left[\begin{array}{l} m\left(v_{k,\tau}\right)R_{p,k1}^{l}\left(\left(\tau-\lambda_k\right)\bmod N_p\right) \\ +m\left(v_{k,\tau}+1\right)R_{p,k1}^{r}\left(\left(\tau-\lambda_k\right)\bmod N_p-N_p\right) \\ +\sum_{\ell=0}^{\infty}d_k(\ell)P_{d,k1}\left(\left(\tau-\lambda_k\right)\bmod N_p\right) \end{array}\right] \quad (18)$$

The second correlation function that is performed using the first correlation function, $V_1(\tau)$, is expressed in Eq. (19).

$$\begin{aligned} V_2(\tau) &= \sum_{v=0}^{N_s-1}m^{*}(v)V_1\left(\tau+vN_p\right) \\ &= \sum_{v=0}^{N_s-1}m^{*}(v)\sum_{k=1}^{K}\left[\begin{array}{l} m\left(v_{k,\tau+vN_p}\right)R_{p,k1}^{l}\left(\left(\tau-\lambda_k\right)\bmod N_p\right) \\ +m\left(v_{k,\tau+vN_p}+1\right)R_{p,k1}^{r}\left(\left(\tau-\lambda_k\right)\bmod N_p-N_p\right) \\ +\sum_{\ell=0}^{\infty}d_k(\ell)P_{d,k1}\left(\left(\tau+vN_p-\lambda_k\right)\bmod N_p\right) \end{array}\right] \end{aligned} \quad (19)$$

In this regard, $v_{k,\tau+vN_p}=v_{k,\tau}+v$, and thus Eq. (19) is as follows.

$$V_2(\tau)=\sum_{v=0}^{N_s-1}m^{*}(v)\sum_{k=1}^{K}\left[\begin{array}{l} m\left(v_{k,\tau}+v\right)R_{p,k1}^{l}\left(\left(\tau-\lambda_k\right)\bmod N_p\right) \\ +m\left(v_{k,\tau}+v+1\right)R_{p,k1}^{r}\left(\left(\tau-\lambda_k\right)\bmod N_p-N_p\right) \\ +\sum_{\ell=0}^{\infty}d_k(\ell)P_{d,k1}\left(\left(\tau-\lambda_k\right)\bmod N_p\right) \end{array}\right] \quad (20)$$

In the case of $\tau=\lambda_1$ and $v_{1,\tau}=0$, when the relative time delay between satellite 1 and other satellites, λ_k, is larger than N_p, $v_k\neq 0$. Thus, Eq. (20) can be expressed as follows.

$$\begin{aligned} V_2(\lambda_1) &= \sum_{v=0}^{N_s-1}m^{*}(v)\left[m(v)R_{p,11}^{l}(0)+m(v+1)R_{p,11}^{r}\left(-N_p\right)\right]+\sum_{\ell=0}^{\infty}d_1(\ell)P_{d1}(0) \\ &+\sum_{v=0}^{N_s-1}m^{*}(v)\sum_{k=2}^{K}\left[\begin{array}{l} m\left(v_{k,\tau}+v\right)R_{p,k1}^{l}\left(\left(\lambda_1-\lambda_k\right)\bmod N_p\right) \\ +m\left(v_{k,\tau}+v+1\right)R_{p,k1}^{r}\left(\left(\lambda_1-\lambda_k\right)\bmod N_p-N_p\right) \\ +\sum_{\ell=0}^{\infty}d_k(\ell)P_{d,k1}\left(\left(\lambda_1-\lambda_k\right)\bmod N_p\right) \end{array}\right] \end{aligned} \quad (21)$$

If the secondary code is the Zadoff-Chu sequence, it has characteristics shown in Eq. (22).

$$\begin{aligned} & \sum_{v=0}^{N_s-1}m^{*}(v)m\left(v_{k,\tau}+v\right)=0 \\ & \sum_{v=0}^{N_s-1}m^{*}(v)m\left(v_{k,\tau}+v+1\right)=0 \end{aligned} \quad (22)$$

Using Eqs. (6, 22), Eq. (21) is calculated as follows.

$$\begin{aligned} V_2(\lambda_1) &= \sum_{v=0}^{N_s-1}m^{*}(v)m(v)R_{p,11}^{l}(0) \\ &+\sum_{v=0}^{N_s-1}m^{*}(v)\sum_{k=2}^{K}\left[\sum_{\ell=0}^{\infty}d_k(\ell)P_{d,k1}\left(\left(\lambda_1-\lambda_k\right)\bmod N_p\right)\right] \end{aligned} \quad (23)$$

The $m(v)$ in Eq. (23) is a complex code type mentioned in Eq. (1). Thus, the inphase component and quadrature component that constitute a complex code value need to be transmitted by being included in the inphase component and quadrature component of the carrier. This signal cannot be transmitted using the general BPSK modulation technique, and a receiver channel using the QPSK modulation technique needs to be organized. In the case of the BPSK modulation technique, two correlator channels (I and Q) are needed; but for the signal acquisition of the proposed signal, four correlator channels (Ii, Iq, Qi, and Qq) are required.

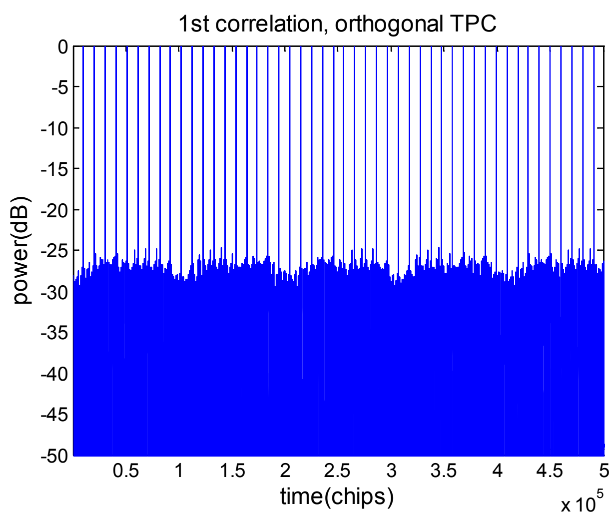

Fig. 5. First correlation result of orthogonal TPC.

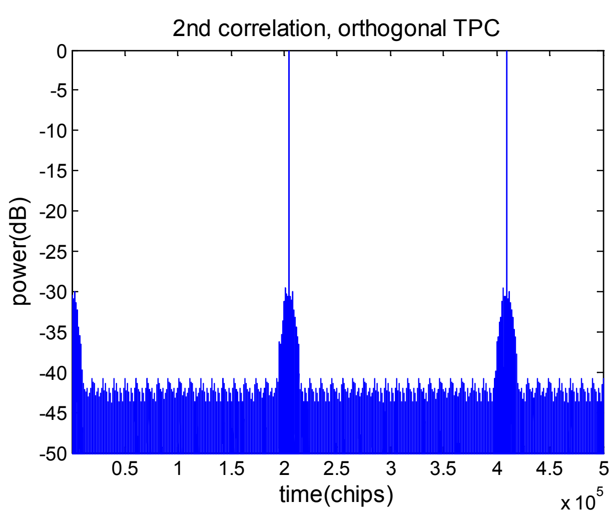

Fig. 6. Second correlation result of orthogonal TPC.

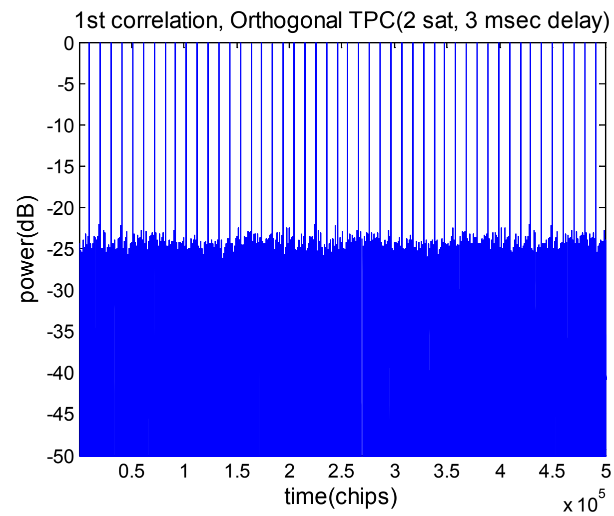

Fig. 7. First correlation result of orthogonal TPC (2 satellite signals relative delay of 3 ms).

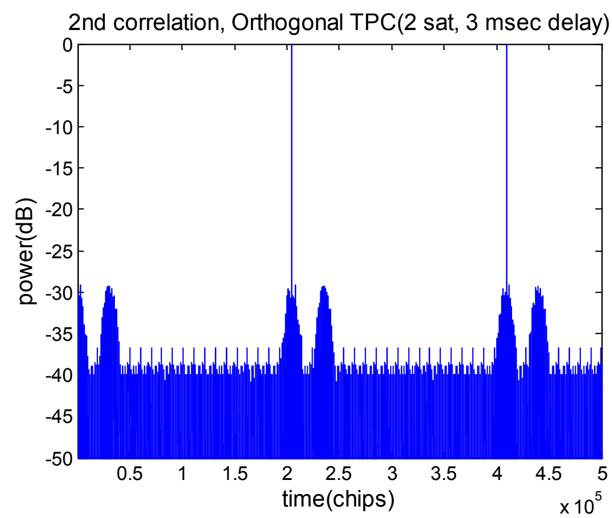

Fig. 8. Second correlation result of orthogonal TPC (2 satellite signals relative delay of 3 ms).

Fig. 5 shows the first correlation result of the navigation signal based on OTPC. It is a case where $K=1$ in Eq. (18); and based on one satellite signal, despreading was performed using the primary code of the satellite signal. Fig. 6 shows the result of despreading using the secondary code from the result of Fig. 5, and it presents the result of Eq. (23) in a figure. There was an interference effect of about -41 dB, compared to the correlation result where only TPC exists. However, the correlation characteristics are outstanding compared to the TC of GALILEO E5a-I which has a side lobe of up to about -14 dB considering the difference from the main lobe, and it is expected that the interference effect on the other satellite signal constituting the same system would be small. If there are two satellite signals constituting the same system that are received with a time delay of 3 ms, it corresponds to a case where $K=2$ in Eq. (18). Fig. 7 shows the result of despreading using the known primary codes when two satellite signals are received with a relative time delay of 3 ms assuming that the primary codes of the two satellite signals are known. Fig. 8 shows the result of despreading using the secondary code from the result of Fig. 5, where the interference effect of only about -37 dB was observed.

Based on the above results, it was found that the navigation signal based on OTPC was free from the interference effect between satellite signals constituting the same system of TPC. To examine the robustness to frequency offset that was suggested as another advantage of TPC, the ambiguity function of the navigation signal based on OTPC was observed as shown in Fig. 9.

Fig. 9 shows the result of the despreading of one navigation signal based on OTPC using Eq. (23) when there

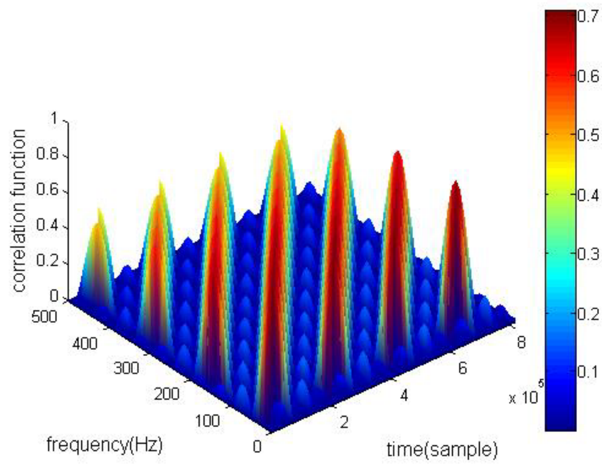

Fig. 9. Ambiguity function of orthogonal TPC.

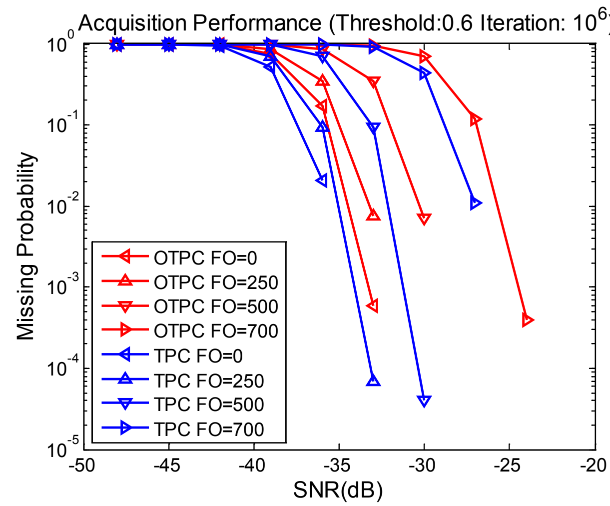

Fig. 10. Signal acquisition performance of orthogonal TPC.

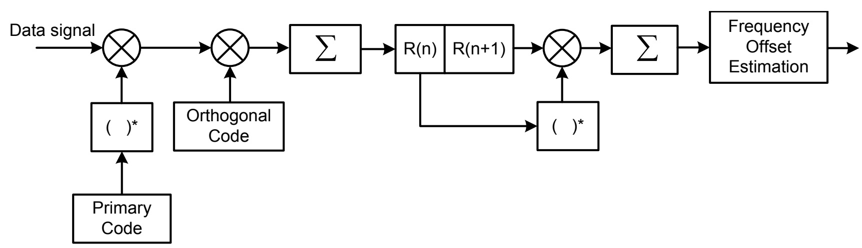

Fig. 11. Frequency offset estimation method.

was a frequency offset of 0 to 500 Hz. As the frequency offset increased, the despreading result value decreased; but although there was a frequency offset, there was always a peak value on the time axis. In other words, even though there is a frequency offset of 500Hz, long-time integration (20 ms) is possible without compensating this error.

In Kim & Ahn (2013), the signal acquisition performances for the TC of GALILEO E5a-I and TPC were compared when there was a frequency offset. In the case of signal acquisition from the received signal through a long-time integration (20 ms), the TC could not perform signal acquisition when there was a frequency offset of 25 Hz, while the TPC had a missing probability of 10^{-2} at a signal-to-noise ratio of -35 dB when there was a frequency offset of 250 Hz. This indicates that when signal acquisition is performed through long-time integration in a weak signal environment, the existing GALILEO E5a-I TC is capable of signal acquisition only when the frequency offset is less than 10 Hz, and the TPC is capable of signal acquisition although the frequency offset is more than 250 Hz. Fig. 10 shows the result of the missing probability when the 20 ms integration result was normalized to a TPC length of 204,600 for signal acquisition and it was considered a successful signal acquisition when the square of the absolute value was above a threshold value of 0.6. In this regard, OTPC is the orthogonal tiered polyphase code, TPC is the tiered polyphase code, and FO is the frequency offset. The OTPC showed a performance difference of about 3 dB compared to the TPC. However, the strength of a signal decreases by $\sqrt{1/2}$ during channel division, and thus it showed the same performance while having no interference effect.

4.2 Frequency Offset Estimation

For TPC where the starting position of a primary code that is received at 1 ms intervals through signal acquisition can be accurately known but there is a limitation in frequency offset estimation for figuring out the starting position of a secondary code that is repeated at 20 ms intervals as mentioned in Chapter 2, it was shown that the frequency offset could be estimated in a synchronization process by adding a data channel through orthogonality. Fig. 11 shows the frequency offset estimation method using a data channel. After signal acquisition, the receiver can figure out the starting point of the primary code based on the data channel. For the result obtained by the despreading of the primary code of the data channel, $R(n)$, the frequency offset is estimated using the delay and multiply technique.

The equation for frequency offset estimation after separating pilot and data using an orthogonal code can be

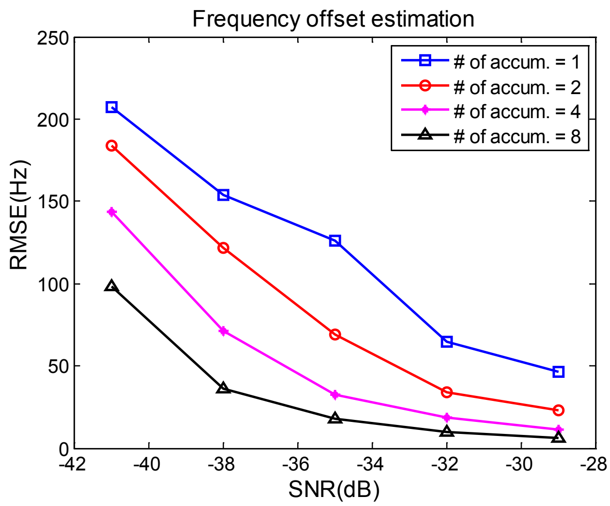

Fig. 12. Frequency offset estimation performance.

expressed as Eq. (24).

$$F(\tau)=\sum_{n=0}^{N_p-1}C_{p,k}(n+\tau)\cdot e^{j2\pi\Delta f(n+\tau)T_s}\cdot C_{p,k}(n)$$
$$=\sum_{n=0}^{N_p-1}\left|C_{p,k}(n)\right|^2 e^{j2\pi\Delta f(n+\tau)T_s}$$
$$F(\tau+N_p)\cdot F^*(\tau)=\sum_{n=0}^{N_p-1}\left|C_{p,k}(n)\right|^2 e^{j2\pi\Delta f N_p T_s} \quad (24)$$

Fig. 12 shows the frequency estimation performance using the primary code of the data channel. When the average receiving power of the signal was assumed to be -130 dBm, the bandwidth to be 20.46 MHz, the thermal noise to be -174 dBm/Hz, and the noise figure to be 6 dB, the operating point of the receiver was -35 dB based on the signal-to-noise ratio. To obtain a frequency offset of less than 25 Hz at -35 dB, the delay and multiply process result values need to be accumulated eight times. If the frequency offset is narrowed within a range of less than 25 Hz through the data channel, frequency offset compensation is enabled using the TPC of the pilot channel, and thus more precise frequency offset estimation is possible. This indicates that the structure of the navigation signal based on OTPC has no interference effect, has signal acquisition performance that is robust to frequency offset, and is capable of frequency offset estimation using a general method after signal acquisition. In addition, by separating pilot/data channels, navigation signals can be transmitted along with precise signal tracking.

5. CONCLUSIONS

In this study, a navigation signal based on TPC with a structure that can separate pilot/data channels using an orthogonal code and can estimate frequency offset was proposed. The proposed signal has no interference effect between satellite signals constituting the same system of TPC, and is robust to frequency offset. Also, it is capable of frequency offset estimation using a data channel based on the delay and multiply technique which is a general frequency offset estimation algorithm, overcoming the disadvantage that a frequency offset of more than ±25 Hz cannot be estimated in a signal acquisition structure with a coherent wide integration interval using TPC. Based on correlation characteristics, it was shown that the navigation signal generated through orthogonalization maintained robustness to interference effect and frequency offset, which is the advantage of TPC. Also, it was found that the signal acquisition performance using a wide correlation interval through a pilot channel in an environment with a frequency offset was also identical. It is expected that the ambiguity of the starting position of a secondary code, which has been problematic during TPC signal acquisition when there is a frequency offset, would be resolved with the development of hardware. However, TPC is a complex code type, rather than a binary code that is used in an existing satellite navigation system. Therefore, the amount of calculation could increase in a satellite signal generation part and a receiver local signal generation part, and it could be operated in the nonlinear interval of a high power amplifier since the constant envelop characteristic cannot be satisfied. Thus, additional studies for overcoming this issue will be performed in the future.

ACKNOWLEDGMENTS

This work has been supported by the National GNSS Research Center Program of the Defense Acquisition Program Administration and the Agency for Defense Development.

REFERENCES

China Satellite Navigation Office 2013, BeiDou Navigation Satellite System Signal In Space Interface Control Document Open Service Signal (Version 2.0), BDS-SIS-ICD-2.0

Dunn, M. J. 2013, Navstar GPS Space Segment/User Segment L5 Interfaces, IS-GPS-705D

European Union 2010, Galileo Open Service Signal in Space Interface Control Document, OS SIS ICD Issue 1.1

Kim, J. B. 2014, A Study on GNSS Ranging Signal Structure Based On The Tiered Polyphase Code for Improving the Acquisition Performance Under Weak Signal Environment, PhD Thesis, Chungnam National University, South Korea

Kim, J. B. & Ahn, J. M. 2013, Acquisition Performance of Tiered Polyphase Code based GNSS Signal, The Journal of Korean Institute of Communications and Information Sciences, 38A, 970-972. http://dx.doi.org/10.7840/kics.2013.38A.11.970

Kim, J. B., Lee, J., Park, D., Kim, K. J., Song, K., et al. 2014, Cross-correlation interference-free tiered polyphase codes for GNSS signal design, Electronics Letters, 50, 218-219. http://dx.doi.org/10.1049/el.2013.2566

Yang, C., Hegarty, C., & Tran, M. 2004, Acquisition of the GPS L5 signal using coherent combining of I5 and Q5, in Proc. of ION GNSS, 17th International Technical Meeting, Long Beach, CA, Sept. 2004, pp.2184-2195. https://www.ion.org/publications/abstract.cfm?jp=p&articleID=5902

Zou, D., Deng, Z., Huang, J., Liu, H., & Yang, L. 2009, A study of Neuman Hoffman codes for GNSS application, in 2009 WiCom'09. 5th International Conference, Beijing, Sep. 2009. http://dx.doi.org/10.1109/WICOM.2009.5305353

Jewon Lee received the Master's degree in Information Communication from Chung-nam National University in 2013. His research interests include satellite navigation and GNSS signal processing.

Jeong-been Kim received the Doctor's degree in Information Communication from Chung-nam National University in 2014. His research interests include satellite navigation and GNSS signal processing

Kap-Jin Kim received the Master's degree in Control & Instrumentation from Han-Yang University in 1997. His research interests include satellite navigation and GNSS signal processing.

Ki-Won Song received the Doctor's degree in Electronics from Chung-nam National University in 2002. His research interests include satellite navigation and GNSS signal processing.

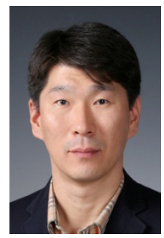

Jae Min Ahn received the Doctor's degree in Electrical and Electronic from KAIST in 1994. His research interests include Physical session of Next-Generation mobile communication and Radio Resource management.